C. H. Whitlock
e-mail: c.h.whitlock@larc.nasa.gov

D. E. Brown

W. S. Chandler

R. C. DiPasquale

Nancy A. Ritchey

Science Applications International Corp.,
One Enterprise Parkway, Suite 300,
Hampton, VA 23666-5845

Shashi K. Gupta
e-mail: s.k.gupta@larc.nasa.gov

Anne C. Wilber

Analytical Services & Materials, Inc.,
One Enterprise Parkway, Suite 300,
Hampton, VA 23666-5845

David P. Kratz
e-mail: d.p.kratz@larc.nasa.gov

Paul W. Stackhouse

NASA Langley Research Center,
Hampton, VA 23681-0001

Global Surface Solar Energy Anomalies Including El Niño and La Niña Years*

Weather anomalies that increase clouds influence the reliability of both renewable energy and building environmental-control systems. Non-grid solar power systems may run out of capacity for such items as communications electronics, flood-warning stream gages, refrigerators, and small village power systems. This paper provides 1×1-degree resolution global maps that identify those regions which experienced large abnormal solar energy during a 10-year period. A source is identified where specific values for maximum year-to-year variability can be obtained in regions where ground-site measurements do not exist. The information may aid in the selection of safety factors for solar power systems. [DOI: 10.1115/1.1384570]

Introduction

This paper synthesizes past events in an attempt to define the general magnitude, duration, and location of large surface solar anomalies over the globe. Surface solar energy values are mostly a function of solar zenith angle, cloud conditions, column atmospheric water vapor, aerosols, and surface albedo. For this study, solar and meteorological parameters for the 10-yr period July 1983 through June 1993 are used. These data were generated as part of the Release 3 Surface meteorology and Solar Energy (SSE) activity under the NASA Earth Science Enterprise (ESE) effort. Release 3 SSE [1] uses upgraded input data and methods relative to previous releases. Cloud conditions are based on recent NASA Version-D International Satellite Cloud Climatology Project (ISCCP) global satellite radiation and cloud data [2]. Meteorological inputs are from Version-1 Goddard Earth Observing System (GEOS) reanalysis data that uses both weather station and satellite information [3]. Aerosol transmission for different regions and seasons are for an "average" year based on historic solar energy data from over 1000 ground sites courtesy of Natural Resources Canada (NRCan) at [4]. These data are input to a new Langley Parameterized Shortwave Algorithm (LPSA) that calculates surface albedo and surface solar energy. That algorithm is an upgraded version of the "Staylor" algorithm [5-7]. Calculations are performed for a 280×280 km equal-area grid system over the

---

globe based on 3-hourly input data. A bi-linear interpolation process is used to estimate data output values on a 1 × 1 degree grid system over the globe.

Maximum anomalies are examined relative to El Niño and La Niña events in the tropical Pacific Ocean. Maximum year-to-year anomalies over the globe are provided for a 10-year period. The data may assist in the design of systems with increased reliability. It may also allow for better planning for emergency assistance during some atypical events.

Comparison of Satellite Insolation with Ground Measurements

Historical ground measurements were obtained from Natural Resources.Canada's CANMET Energy Diversification Research Laboratory (CEDRL) and the National Renewable Energy Laboratory (NREL). The 30-year average RETScreen™ database from CEDRL contains temperature, wind, humidity, and solar energy data from more than 1000 sites [4]. NREL distributes the World Radiation Data Center (WRDC) monthly surface solar energy measurements for 1195+ sites from 1964 through 1993 [8]. All ground stations were not operating for every year in either data set. Therefore, various years of data contained different combinations of ground site locations. When more than one ground measurement station was located in a grid cell, the ground measurements were averaged for comparison to the SSE data.

It is generally believed that quality measured ground data are more accurate than satellite-derived values. Unfortunately, measurement uncertainties are not precisely known for either ground site data set. For this reason, SSE differences from ground measurements are considered as estimates of uncertainty.
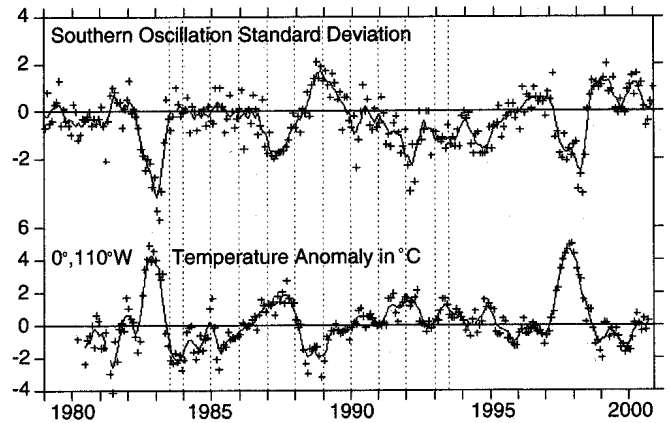
Table 1 Estimates of Insolation RMS Uncertainty Including Bias

Time Period	Global Interior Regions WRDC Site Data	Global Coastal Regions WRDC Site Data	Global All Regions RETScreen Site Data
Near-Average Years			
1983-2nd Half	11.7%	12.9%	
1984	13.8%	13.1%	13.9%
1986	13.5%	12.5%	13.1%
1986	13.1%	13.7%	12.6%
1990	15.5%	15.4%	13.4%
El Niño Years			
1987	14.5%	14.6%	
1991	17.0%	15.9%	
1992	15.4%	13.7%	
1993-1st Half	14.9%	15.4%	
La Niña Years			
1988	14.8%	13.8%	
1989	14.9%	13.9%	

Fig. 1 Time histories of Southern Oscillation Index and equatorial water temperature deviation at 110 deg West

Following usual industry standards, estimated uncertainty is the Root-Mean-Square (RMS) difference when large sample sizes exist and statistical correlation has been performed. Bias is included in the RMS values. Estimated uncertainties over the 10-year data period are given in Table 1 from [9]. Slight RMS increases during El Niño and La Niña years may be caused by localized abnormal aerosols (i.e., smoke and pollution) or water vapor as a result of

droughts and wind changes that might not have been detected by satellite or reanalysis data. Average bias differences for the WRDC data set range from −2.0% to +3.3% depending on the year. Thirty-year average RETScreen data bias differences range from +1.0% to +2.5% depending on the near-average year. Bias and RMS results suggest that the Release 3 satellite-based values follow similar geographical and time-history trends as ground-site
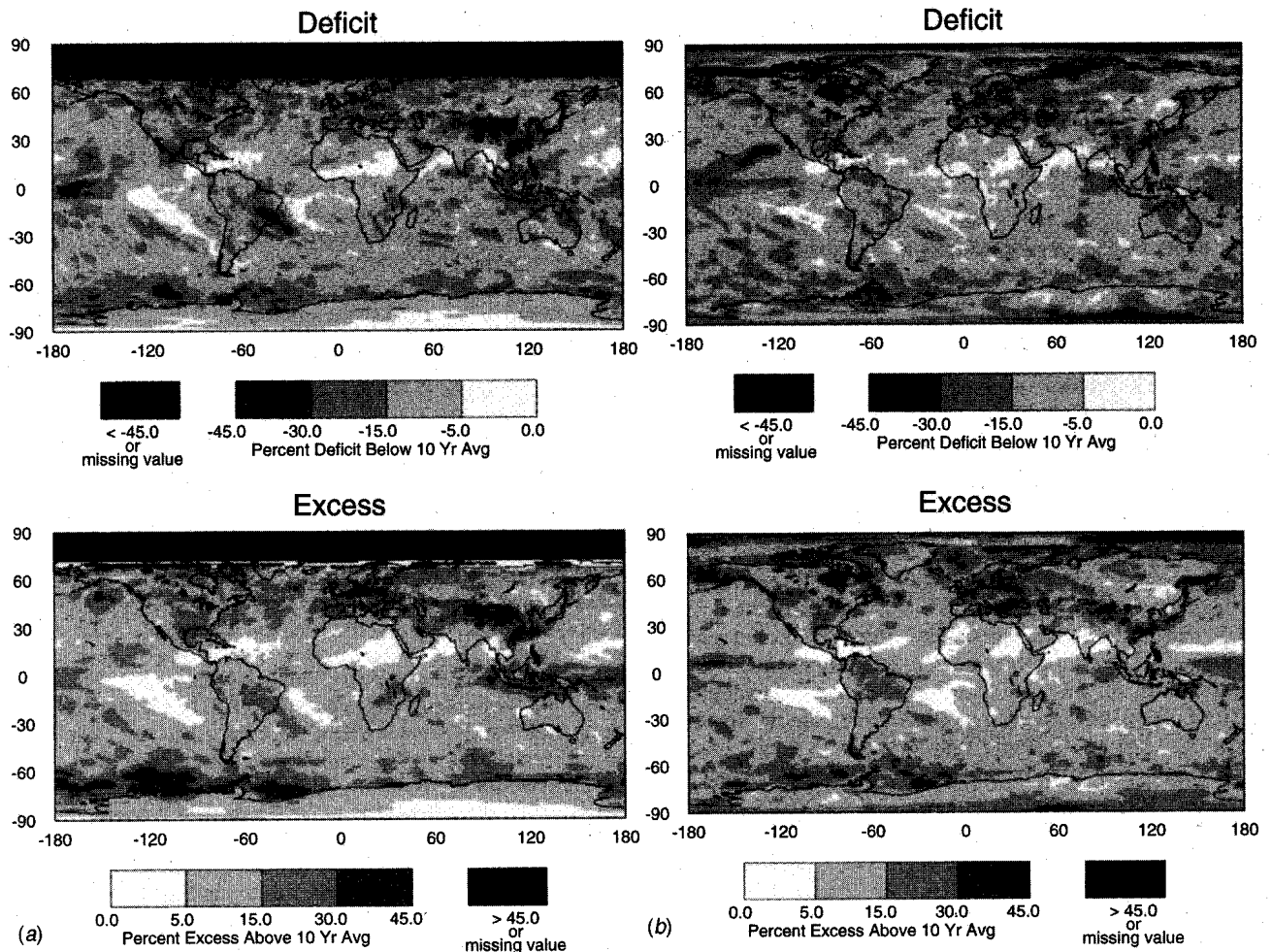
Fig. 2 (a) January deficit and excess insolation relative to 10-yr average; (b) March deficit and excess insolation relative to 10-yr average.
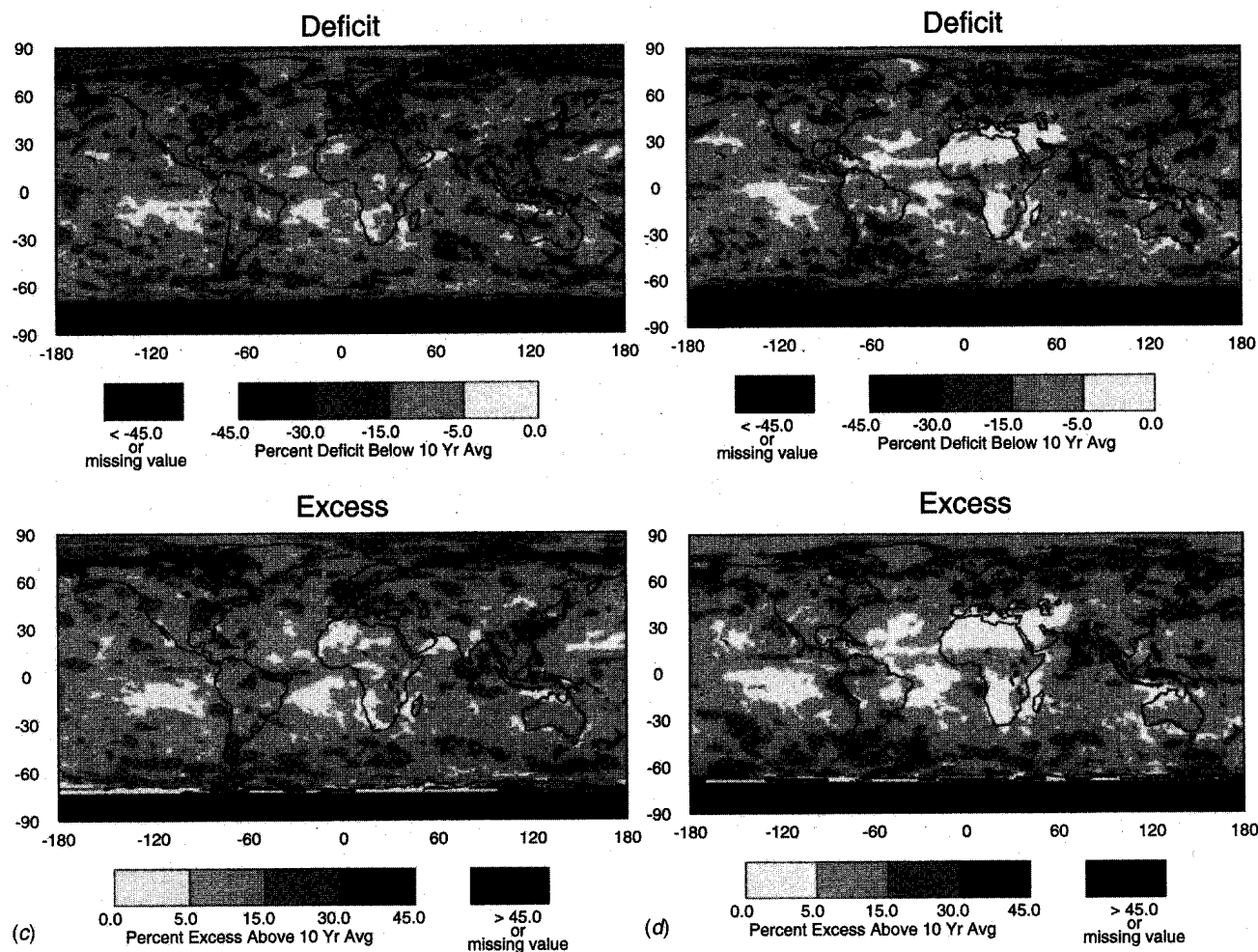
Fig. 2 (c) **May deficit and excess insolation relative to 10-yr average;** (d) **July deficit and excess insolation relative to 10-yr average.**

measurements. Release 3 SSE results may be useful to energy system designers in remote regions without quality ground site measurements.

El Niño/La Niña Events

Under normal conditions, easterly trade winds near the equator in the tropical Pacific cause a warm water pool to form in the west Pacific. This creates sea surface temperatures about 8°C higher in Indonesia than those off the coast of Ecuador.

When El Niños exist, weaker than normal trade winds occur in the central and western Pacific. The warm water pool drifts eastward warming the atmosphere over the eastern Pacific causing changes in atmospheric circulation that affect regions in other parts of the globe. In the December through January period, warmer-than-normal temperatures are reported to occur in the northeast U.S., eastern Canada, western Canada, north central U.S., Japan, eastern and southern China, Burma, India, southern Australia, and southeast Brazil. Droughts occur in Indonesia. Unusually wet conditions may occur in Peru and Ecuador. June through August anomalies typically cause droughts in India, Indonesia, and eastern Australia. Wetter-than-normal weather occurs in the northwestern U.S. and northern Chile [10].

Under La Niña conditions, stronger than normal trade winds push the warm water pool further west which allows colder water from South America to flow further west along the Equator. Changing both the warm and cold water locations again changes

atmospheric heating locations and circulation patterns in many regions of the globe. La Niña impacts are believed to be opposite those from El Niño on a global scale.

Scientists have discovered a correlation of the difference in surface atmospheric pressure between Darwin, Australia and Tahiti and the seesawing of the warm water pool between the eastern and western sides of the tropical Pacific Ocean. The Southern Oscillation Index (SOI) is the Tahiti minus Darwin pressure difference standardized by the 1951 to 1980 mean annual standard deviation. It is usually correlated with surface water temperature measurements on the Equator at 110 degrees West. Negative values of SOI usually indicate warmer-than-normal El Niño water conditions, and positive values suggest cooler-than-normal La Niña water.

Owners and operators of renewable energy systems can now obtain near-real-time status of both the 110 degree West water temperature and the SOI [11]. Forecasts of oncoming events are also available [12]. Little information is available on changes in cloud cover and solar energy reaching the Earth's surface, however.

Surface Solar Energy During Near-Average and El Niño/La Niña Years

El Niño and La Niña events vary in strength, timing, and duration. The magnitudes of SOI and water temperature deviation are shown in Fig. 1, courtesy of [11]. If either or both indicators differ from zero by more than 0.5 (or 0.5°C), an El Niño or La Niña may
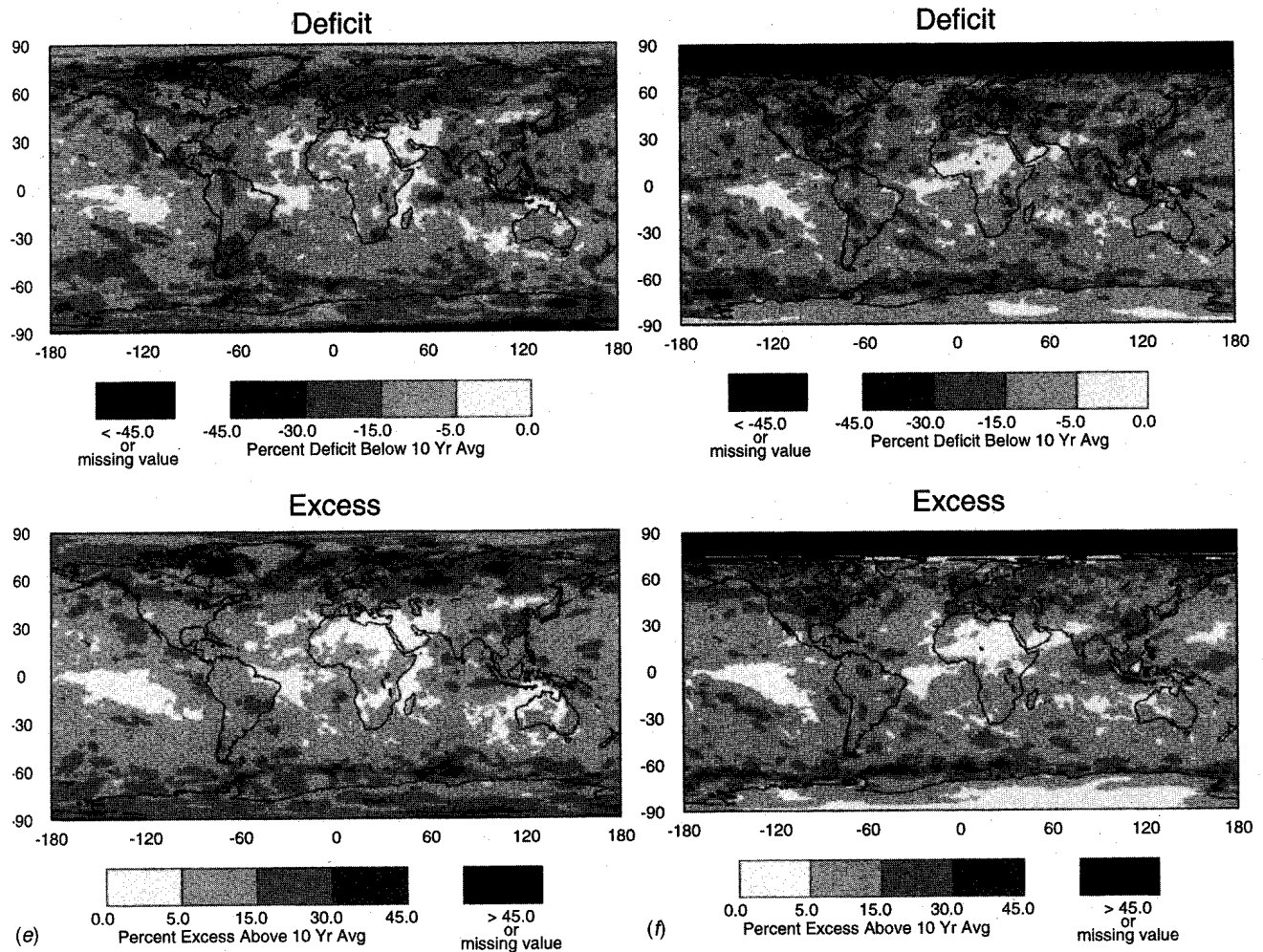
Fig. 2 (*e*) **September deficit and excess insolation relative to 10-yr average;** (*f*) **November deficit and excess insolation relative to 10-yr average.**

be occurring. The time period of the SSE data used in this study are shown by the initial and final vertical dashed lines. Other lines show the beginning of each year. Note that the unusual high-strength El Niños in 1982-1983 and 1997-1998 are not included in the present SSE data set. Appropriate satellite data are not yet available for these two time periods.

The Fig. 1 graph's solid lines represent 5-month running means that do not always indicate the same thing is happening. There appear to be time lags with either parameter leading the other by some months at various time periods. Near-average years based on the SOI definition may contain either an El Niño or a La Niña based on temperature variation. This inconsistency appears to be carried over into surface solar energy values. Two remote regions where El Niños and La Niñas are known to have a strong influence are examined below:

1. In the above El Niño scenarios, winter droughts occur in Indonesia and northern Australia. This study finds that surface solar energy does not always follow the expected pattern of fewer clouds. Indonesia had both 20% more solar energy (January, 1992) and 20% less solar energy (January, 1987) for the same values of SOI (−2) and 110-deg West temperature deviation (+2°C).

2. The above El Niño scenarios suggest large amounts of winter rain in western South America, suggesting more clouds. The same ±20% opposite solar energy variation occurs in western South America during the above two January El Niño dates.

Reviews of individual monthly solar insolation maps for the globe show similar inconsistency in other regions for the mid-strength El Niños and La Niñas contained in this particular 10-yr data period. Additional work is required to develop more reliable indicators of surface solar energy variations related to El Niño and La Niña events. Those studies are suggested when appropriate satellite data for the high-strength El Niños in 1982-1983 and 1997-1998 become available. It appears safer for system designers and plant operators to continue decisions based on maximum anomalies at this time.

10-Year Maximum Solar Energy Anomalies

Figures 2(*a*) through 2(*f*) show maximum surface solar energy deficits and excesses relative to 10-year average values over the globe. Deficits are given as the percent of solar energy that was not available relative to the expected average value for the month. Excess is the percent above the monthly average expected. Maps for every other month are shown for reasons of brevity. The maps show regions of unusual stability (±5% white areas) in spite of weather events such as El Niños and La Niñas. Most of the globe appears to have year-to-year variability within ±15%. Many regions have higher variability for only a few months that may or may not be critical to a particular solar-energy system. There are a few land regions with very large variability (>45%). These are the Arctic coasts, central China, portions of Europe, and small regions in Canada.

System designers may use Fig. 2 for quick assessment of the

general magnitude of maximum year-to-year variability in various regions of the globe. Values for a specific location may be obtained as described below.

The NASA Release 3 SSE Website

More precise information for specific locations can be obtained from the NASA Release 3 SSE website [1]. Meteorology, wind, surface albedo, and surface solar energy parameters can be obtained for each 1-degree cell over the globe subject to uncertainties described in both the Methodology and Accuracy sections of the website. Monthly average, maximum, minimum, 1987 El Niño, and 1988 La Niña surface solar energy values are given for each cell. These may be useful for preliminary selection and sizing of systems. Within-month information is also provided that is useful for the design of both backup systems and storage of surplus product. Maximum consecutive-day deficits and surpluses are available in several forms including the Equivalent No-Sun (or Black) Day design parameter. These values are obtained based on 3-hourly NASA cloud and meteorology information over the entire 10-yr period.

Concluding Remarks

Atypical events are known to occur for extended periods of time. Anomalies that increase clouds, aerosols, or water vapor may influence the reliability of both renewable energy and building environmental-control systems. This paper provides global maps that identify those regions that experienced significant variation in the surface solar energy resource over a 10-yr period. The maps are useful for quickly estimating the order-of-magnitude of maximum variability. A source for more detailed information at specific locations has been provided.

References

[1] Release 3 SSE data can be obtained from ⟨http://eosweb.larc.nasa.gov/sse⟩.
[2] ISCCP data can be obtained through ⟨http://isccp.giss.nasa.gov⟩ and/or ⟨http://eosweb.larc.nasa.gov⟩.
[3] GEOS data can be obtained from ⟨http://dao.gsfc.nasa.gov⟩.
[4] RETScreen™ data can be obtained from ⟨http://retscreen.gc.ca⟩.
[5] Darnell, W. L., Staylor, W. F., Ritchey, N. A., Gupta, S. K., and Wilber, A. C., 1996, "Surface Radiation Budget: A Long-Term Global Dataset of Shortwave and Longwave Fluxes," American Geophysical Union, ⟨http://www.agu.org/eos_elec/95206e.html⟩.
[6] Gupta, S. K., Ritchey, N. A., Wilber, A. C. Whitlock, C. H., Gibson, G. G., and Stackhouse, P. W., Jr., 1999, "A Climatology of Surface Radiation Budget Derived From Satellite Data" J. Clim., **12**, pp. 2691–2710.
[7] Whitlock, C. H., Charlock, T. P., Staylor, W. F., Pinker, R. T., Laszlo, I., Ohmura, A., Gilgen, H., Konzelmann, T., DiPasquale, R. C., Moats, C. D., Le Croy, S. R., and Ritchey, N. A., 1995, "First Global WCRP Surface Radiation Budget Data Set," Bull. Am. Meteorol. Soc., **76**, pp. 905–922.
[8] WRDC data can be obtained from ⟨http://wrdc-mgo.nrel.gov⟩.
[9] Whitlock, C. H., Brown, D. E., Chandler, W. S., DiPasquale, R. C., Meloche, N., Leng, G. J., Gupta, S. K., Wilber, A. C., Ritchey, N. A., Carlson, A. B., Kratz, D. P., and Stackhouse, P. W., 2000, "Release 3 NASA Surface Meteorology and Solar Energy Data Set for Renewable Energy Use," Proc., Rise and Shine 2000, the 26th Annual Conf. of the Solar Energy Society of Canada Inc. and Solar Nova Scotia, October 21-24, Halifax, Canada, ⟨http://www.chebucto.ns.ca/Technology/RS2000/papers/0621-06/⟩.
[10] El Niño and La Niña background information can be obtained from ⟨http://iri.ldeo.columbia.edu/climate/dictionary/enso/impacts.html⟩, ⟨http://www.pmel.noaa.gov/toga-tao/el-nino-story.html⟩, ⟨http://www.pmel.noaa.gov/toga-tao/la-nina-story.html⟩, and ⟨http://iri.ldeo.columbia.edu/climate/dictionary/enso/ensoevent.html⟩.
[11] Near-real-time status of El Niño and La Niña indicators can be obtained at ⟨http://www.pmel.noaa.gov/toga-tao/gif/daily/soi_110w_80.gif⟩.
[12] Forecasts of oncoming events can be obtained at ⟨http://www.pmel.noaa.gov/toga-tao/el nino/forecasts.html⟩.